AIAA JOURNAL
Vol. 46, No. 8, August 2008

Bimodal Buckling of Optimized Truss-Lattice Shear Panels

P. A. Williams,* H. A. Kim,† and R. Butler‡
University of Bath, Bath, England BA2 7AY, United Kingdom

DOI: 10.2514/1.29034

A truss-lattice panel is modeled under shear loading, up to and beyond the critical buckling load. Nondimensional buckling loads and corresponding buckling mode shapes are obtained for such panels with increasing numbers of diagonally placed internal struts. A method for minimum-mass optimization of the truss lattice is given, based upon simultaneous in-plane and out-of-plane buckling. The finite element method is applied to examine the buckling performance and postbuckling stability. The postbuckling response of the optimized truss lattice is shown to be stable in all cases. The advantages of using the truss-lattice structure are demonstrated by comparing the volume requirements with those of a conventional continuous shear panel, based on the load carried and the buckling capabilities. It is shown that although the continuous shear panel is more efficient for heavy load applications, the truss lattice offers potential weight savings when lighter loads are applied.

Introduction

SHEAR panels are used extensively within aerospace structures, forming components such as the ribs and spars of an aircraft wing. Their design has conventionally taken the form of continuous webs, although this paper will consider the use of optimized truss-lattice panels as a lightweight alternative structure.

The semimonocoque configuration of aircraft design has a continuous aluminum skin with integral stiffening [1,2]. The skin is subjected to shear loading and develops short-wavelength buckling beyond the critical buckling load [3,4]. Loading in excess of the critical buckling load is carried predominantly in tension, and the subsequent diagonal tension field provides a stable and fail-safe design. A thin web thickness allows postbuckling to occur, significantly reducing the structural weight of the component. Such a continuous structure can be used to contain payload and fuel and can be easily inspected for damage. Also, the stress level of the continuum is generally lower than that of discrete structures, and hence the continuum has better fatigue performance.

The truss-lattice panel considered in this paper is a deep beam with discrete horizontal, vertical, and diagonal truss members, arranged as in Fig. 1. When subject to shear, the stiff horizontal and vertical members support axial and bending loads, and the internal lattice of diagonal struts resist shear deformation. Such a configuration has been commonplace within structural design for many years. It is similar to the three-dimensional space frame and geodetic structures used widely in civil engineering [5,6] and also to great effect by Barnes Wallis in his design of the Wellington Bomber. In the case of the Wellington, an aluminum alloy truss provided a stiff and lightweight structure, with a canvas covering to provide the aerodynamic surface [1].

Such truss structures are typically considered to be unbuckled, as there has been only limited investigation conducted into their postbuckling behavior and optimization, and hence current applications do not exploit their postbuckled strength. Notable work has been conducted recently on periodic two-dimensional [7] and three-dimensional [8,9] lattice designs. The members are generally assumed to be pin-jointed for the buckling analysis and are aligned to give optimum performance for a variety of different load cases. The high strength-to-weight ratio of these truss structures makes them attractive for aerospace applications. One configuration features a truss structure as the core of a sandwich panel, which also has potential to act as heat transfer elements or storage cavities, an additional feature that cannot be achieved with more conventional foam-based fillings. However, the buckling of a member in these lattices can lead to the collapse of the structure [9], and it is well known that an optimized structure can be highly unstable when buckling is considered [10].

It is proposed that, just as the continuous web develops a stable diagonal tension field under pure shear buckling conditions, discrete optimized members within the truss-lattice structure could be arranged to support a similar tension field. Hence, the structure would benefit from the additional postbuckling performance, along with the potential for weight saving. A preliminary investigation of a simple truss-lattice finite element model under a shear load demonstrated that the tensile diagonal member continued to carry the applied load beyond the buckling of the compressive diagonal member [11]. Thus, the truss-lattice configuration exhibited a similar postbuckling behavior to that of a continuous web.

Truss-lattice designs will only be considered if they are more efficient than the existing continuous panels, hence the need for optimization. One of the intuitive optimization criteria for structural stability is the simultaneous-failure-mode approach [12]. It is generally perceived that the unstable interaction of coincident modes in an optimum design leads to "dangerous coupling of modes" and failure by an explosive instability [13,14]. It is shown in [15] that a strong nonlinear interaction occurs between coincident local and overall buckling in a built-up hollow column of constant cross section. The resulting design, sometimes referred to as the "naive optimum," was extremely imperfection-sensitive. However, a recent study [16] analyzed the behavior of an optimized column with a variable (solid) cross section along its length and concluded that the stability during postbuckling was dependent on the rigidity of the support conditions and not inherent to the multimodality of the optimum.

This paper presents an investigation into the buckling and postbuckling behavior of an optimized truss-lattice panel under shear load. The following section introduces the truss-lattice model, which is studied first through eigenbuckling finite element (FE) analysis. The cross-sectional geometry of the diagonal members is then optimized to achieve simultaneous in-plane and out-of-plane buckling, before postbuckling behavior is investigated using nonlinear finite element analysis. A simple dimensional comparison between the truss-lattice structure and the continuum is also

Presented as Paper 2122 at the 48th AIAA/ASME/ASCE/AHS/ASC Structures, Structural Dynamics, and Materials Conference, Honolulu, HI, 23–26 April 2007; received 27 November 2006; revision received 27 September 2007; accepted for publication 6 April 2008.

*Postgraduate Research Student, Department of Mechanical Engineering; P.Williams@bath.ac.uk. Student Member AIAA.

†Lecturer, Department of Mechanical Engineering; H.A.Kim@bath.ac.uk. Member AIAA.

‡Reader, Department of Mechanical Engineering; R.Butler@bath.ac.uk.

presented to highlight the potential benefit of the truss-lattice configuration.

Truss-Lattice Model

Figure 1 represents an example of the truss-lattice structure considered in this paper. The vertical and horizontal members, shown as thick solid lines in Fig. 1, carry compression and bending in a similar way to stiffeners and flanges in a continuous stiffened shear panel. In this paper, we assume that only shear loading is applied to the diagonal lattice members, shown as thin solid lines in Fig. 1, which run at ± 45 deg and are welded at their intersections. This assumption is realistic if the shear panel is thin (or flexible) compared with the surrounding frame. The term *truss lattice* in this case refers to a network of diagonal beams, each rigidly connected at the nodes of intersection (rather than the more typical pin joint). Assuming small displacements up to buckling, the load produces tension in one set of diagonal members and compression in the other, which is analogous to the load distribution within a continuous web under pure shear.

Two intersecting diagonal struts, welded at their center and highlighted in Fig. 2a, constitute one unit (or cell) of the truss lattice. The cell dimension is defined as n, where the number of cells in each model is n^2. Figure 2 hence depicts the four-cell (or $n = 2$) model. We consider a frame around the lattice, consisting of rigid members with pinned corner joints, to which the lattice members have a simply supported connection. Load is applied to the frame at the corners to represent a shear load per unit length (shear flow) q, which is transferred to the members via the frame as a displacement controlled mechanical system. For small displacements, the unbuckled lattice members are each subjected to tensile or compressive loads p, in accordance with

$$p = \frac{P}{n} = \frac{qB}{n\sqrt{2}} \tag{1}$$

The side length B is constant for a given panel, and we will assume here that the panels are square.

The structure buckles in the X–Y plane at the critical value p^c_{zz}, or out-of-plane at p^c_{yy}. These buckling loads can be related to the equivalent Euler buckling load P^E of a pin-ended strut by

$$p^c_{zz} = \rho_{zz} P^E_{zz} \tag{2}$$

$$p^c_{yy} = \rho_{yy} P^E_{yy} \tag{3}$$

where ρ_{yy} and ρ_{zz} are nondimensional buckling loads corresponding to in-plane and out-of-plane buckling of the truss lattice, respectively. The Euler buckling load for a strut of length ℓ with Young's modulus E and second moment of area I is given by

$$P^E = \pi^2 EI/\ell^2 \tag{4}$$

So by relating ℓ to the side length B, the in-plane and out-of-plane Euler loads can be expressed by

$$P^E_{zz} = \frac{2\pi^2 n^2 EI_{zz}}{B^2} \tag{5}$$

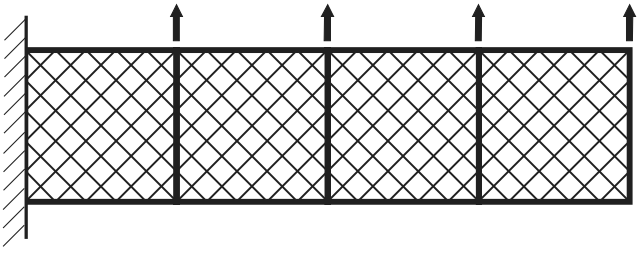

Fig. 1 Example of a truss lattice within an idealized stiffened spar, showing applied loads.

$$P^E_{yy} = \frac{2\pi^2 n^2 EI_{yy}}{B^2} \tag{6}$$

By combining Eq. (1) with Eqs. (2) and (3), the critical values of applied shear flow for in-plane and out-of-plane buckling (q^c_{zz} and q^c_{yy}, respectively) are

$$q^c_{zz} = \frac{\sqrt{2} n \rho_{zz} P^E_{zz}}{B} \tag{7}$$

$$q^c_{yy} = \frac{\sqrt{2} n \rho_{yy} P^E_{yy}}{B} \tag{8}$$

For simplicity, we will assume a rectangular cross section for the struts (see Fig. 2), for which Eqs. (9) and (10) apply:

$$I_{yy} = \frac{bd^3}{12} \tag{9}$$

$$I_{zz} = \frac{b^3 d}{12} \tag{10}$$

The polar second moment of area, J, is given by

$$J = \beta bd^3 \tag{11}$$

where β varies with b/d when considering the angle of twist for a shaft of rectangular cross section with warping effects [17]. The volume of the n^2-cell truss lattice with rectangular struts is then

$$V_L = 2\sqrt{2} nBbd \tag{12}$$

Eigenbuckling Finite Element Analysis

FE analysis is employed to determine the critical buckling load factors ρ_{yy} and ρ_{zz} for a range of cell dimensions. The ABAQUS software [18] is used for the analysis. For convenience, the model shown in Fig. 2a is rotated by 45 deg to align the struts with the conventional XYZ coordinate system. Each strut of length ℓ is modeled with eight 3-dimensional Euler–Bernoulli beam elements, which is sufficient number of elements for the $n = 1$ model to be within 0.01% of the correct buckling load, obtained from the Wittrick–Williams approach [19] (following the mesh convergence study given in [20]). The beam elements can carry the axial compression and tension loads before buckling, as well as the induced bending loads of the deformed mode shapes. This is a postbuckling effect and is examined in more detail in [20].

The frame around the lattice is modeled by beams with very high axial and bending stiffness. The in-plane rotations at the four corners of the frame are released to allow shear deformation of the structure. Nodes along the frame must be solid joints, such that each side of the frame is one rigid member. However, where the lattice meets these nodes along the frame there is a pinned connection, allowing the lattice members to rotate in-plane or out-of-plane. This is implemented in ABAQUS through the use of multipoint constraints [18] between the nodes of the lattice and frame.

Figure 2b depicts an $n = 2$ truss lattice as an example, requiring a total of 128 elements, and shows the constrained global degrees of freedom.

Table 1 gives the nondimensional in-plane and out-of-plane buckling loads, defined in Eqs. (2) and (3), as obtained by eigenvalue analysis from the FE models. These models were validated by applying exact member theory and the Wittrick–Williams algorithm [19]. The half-cell model in Table 1 corresponds to a single compression member, for which the buckling load is the Euler load from Eq. (4).

In calculating the nondimensional buckling loads, the value of $1/3$ is used for β in Eq. (11), which assumes that b/d is large, and hence $J = 4I_{yy}$. However, the out-of-plane modes are sensitive to the torsional rigidity of the members, as they involve some twisting, and

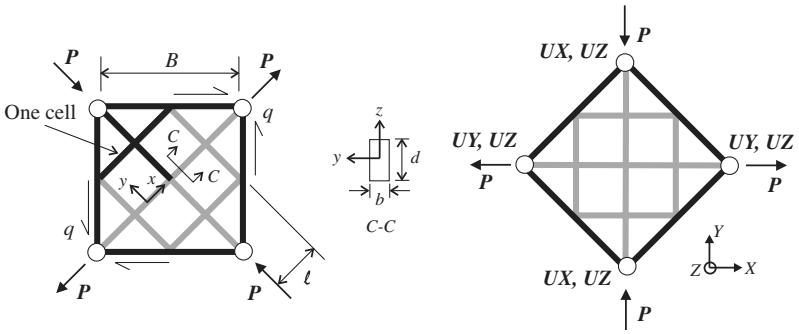

a) b)

Fig. 2 Four-cell $n = 2$ truss-lattice model: a) geometry and loading (shear flow q can be represented by diagonal loads P) and b) finite element model showing translational constraints applied in the global X, Y, and Z axis system at the four pin joints.

so the correct value of J must be used for a given cross section, calculated using the β values from [17] in Eq. (11).

Optimization

For a truss lattice with beams of rectangular section, buckling out-of-plane, the critical load can be maximized by increasing the depth of the beams and hence the out-of-plane second moment of area I_{yy}. However, there is a limit to how far this value can be increased before in-plane buckling occurs, and subsequent increase in the depth of the member will achieve no further gain in buckling load. The requirement of minimum mass selected for the truss-lattice configuration is based upon an optimality criterion of simultaneous-failure modes. This bimodal condition is often viewed as both unstable and unpredictable [15]. However, the truss-lattice configuration considered in this paper is able to carry loads beyond buckling, as discussed in more detail in the following section. This inherent stability of the configuration justifies the application of the simultaneous-failure criterion.

The design variables are the cross-sectional dimensions of the struts. Thus, equating the critical shear flow q^c for in-plane and out-of-plane buckling from Eqs. (7) and (8), gives

$$\rho_{yy} I_{yy} = \rho_{zz} I_{zz} \tag{13}$$

Substituting Eqs. (9) and (10) for a rectangular cross section simplifies to

$$b = d\sqrt{\frac{\rho_{yy}}{\rho_{zz}}} \tag{14}$$

Now, substituting Eqs. (6), (9), and (14) into the general expression for q^c_{yy} given by Eq. (8), we have

$$q^c_{yy} = \frac{\sqrt{2}\pi^2 n^3 E d^4 \rho_{yy}}{6B^3}\sqrt{\frac{\rho_{yy}}{\rho_{zz}}} \tag{15}$$

If the truss lattice is designed to buckle at critical shear flow q^c, then rearranging Eq. (15) gives

$$d = \left(\frac{6q^c B^3}{\sqrt{2}\pi^2 E \rho_{yy} n^3}\sqrt{\frac{\rho_{zz}}{\rho_{yy}}}\right)^{1/4} \tag{16}$$

Table 1 Nondimensional buckling loads for truss lattice of varying cell dimension n

n	ρ_{yy}	ρ_{zz}
1/2	1.000	1.000
1	1.562	1.562
2	0.521	1.729
3	0.384	1.746
4	0.252	1.748
5	0.172	1.744

Substituting Eq. (14) into Eq. (12) gives the expression for the optimum volume V_L:

$$V_L = 2\sqrt{2} n B d^2 \sqrt{\frac{\rho_{yy}}{\rho_{zz}}} \tag{17}$$

Considering Fig. 2 again, the stress in the unbuckled truss-lattice struts is given by

$$\sigma_L = \frac{p}{bd} \tag{18}$$

This may be expressed in terms of the shear flow q (where $q \le q^c$) using Eq. (1), to give

$$\sigma_L = \frac{qB}{\sqrt{2} nbd} \tag{19}$$

Now substituting for the optimum dimensions in Eq. (14),

$$\sigma_L = \frac{qB}{\sqrt{2} nd^2}\sqrt{\frac{\rho_{zz}}{\rho_{yy}}} \tag{20}$$

Hence, combining Eqs. (17) and (20) gives

$$\sigma_L = \frac{2qB^2}{V_L} \tag{21}$$

Figure 3 shows the variation of optimum volume from Eq. (17) with cell dimension n, based on the nondimensional buckling loads in Table 1. The applied shear flow q and side length B are kept constant. Compared with the optimum volume of the $n = 1/2$ model, there is a 43% reduction in volume when an optimized $n = 1$ truss lattice is used and a further 13% reduction when an optimized $n = 4$ truss lattice is used. In other words, the efficiency of the lattice improves with increasing numbers of cells, although beyond $n = 4$, the improvement becomes less significant.

Similarly, Fig. 4 can be obtained from Eq. (20) and Table 1 and shows that the stress in the optimized truss lattice σ_L increases with an increasing number of cells. It can be seen that the stress in the optimized $n = 1$ truss lattice is 77% higher than the stress in the $n = 1/2$ model, whereas in the $n = 4$ truss lattice, it is 129% higher.

Postbuckling Analysis of Optimum Truss Lattice

Truss lattices with optimum cross sections given by Eqs. (14) and (16) are analyzed using a nonlinear FE procedure within the ABAQUS software [18] to observe the postbuckling behavior. The constraints for the eigenbuckling analysis in Fig. 2 are again applied to the model. The buckling mode shapes obtained from the eigenanalysis are depicted in Figs. 5 and 6.

The first out-of-plane buckling mode for the $n = 1$ model, shown in Fig. 5a, is a global mode in the form of a half sine wave with a flattened crest. The first in-plane buckling mode (coincident with the

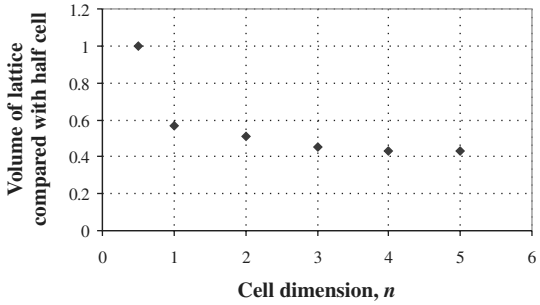

Fig. 3 Optimum truss-lattice volume of cell dimension n for constant shear flow q and side length B.

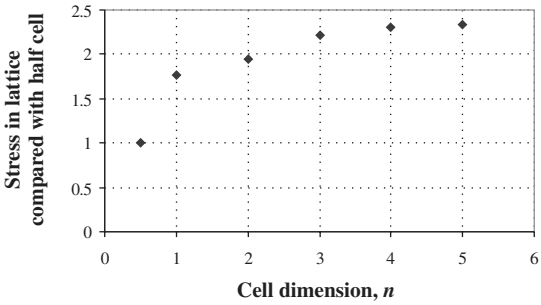

Fig. 4 Stress in optimum truss lattice of cell dimension n for constant shear flow q and side length B.

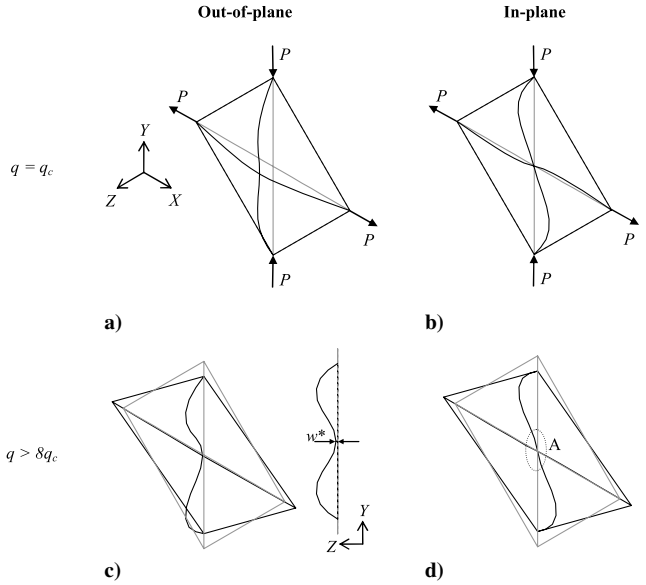

Fig. 5 Critical and postbuckling modes for the $n = 1$ truss lattice.

out-of-plane mode), shown in Fig. 5b, is a local mode in the form of a complete sine wave.

For the $n = 2$ model, the first out-of-plane buckling mode is again a global mode, as shown in Fig. 6a, and takes the form of one-and-a-half sine waves. The middle compression member has a large central deflection in the positive Z direction and a small deflection in the upper and lower sections in the negative Z direction. The in-plane mode in Fig. 6b is once again a local mode, based on two sine waves in the central member.

The modified Riks method is the approach implemented for postbuckling procedures in ABAQUS [18] and is used here to investigate the postbuckling behavior of the optimum truss lattices. The postbuckling load-displacement path is followed by finding the tangent line to the current solution point, stepping a predetermined

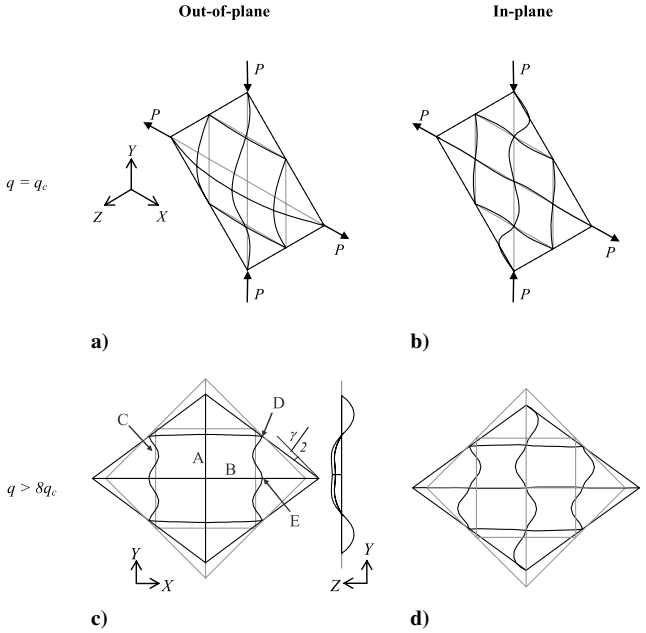

Fig. 6 Critical and postbuckling modes for the $n = 2$ truss lattice.

distance along this line, then searching for equilibrium conditions orthogonal to the end of the step. Further details are given in [18,21]. The method requires an imperfection to initiate the buckling behavior, and hence the critical buckling mode shapes were imported to produce the postbuckling modes in Figs. 5c, 5d, 6c, and 6d. The maximum imperfection used was 0.2% of the length ℓ, which was sufficient to initiate both in-plane and out-of-plane analyses, without inducing large errors to the initial postbuckling results. Although the postbuckling behavior of the truss lattice is nonlinear, the material properties are assumed to be linear throughout.

As the applied load P in the $n = 1$ model increases beyond the critical buckling load, the out-of-plane deflection of the compression strut increases, as shown in Fig. 5c. However, the central deflection is reduced due to the stiffening effect of the tension member. The out-of-plane buckling mode therefore progresses into three half sine waves.

In contrast, the in-plane buckling mode in Fig. 5d remains in the initial mode shape of a complete sine wave. The stiffening effect of the tension member is also noticeable in the central deflection, where it restricts some rotation of the central node, marked region A of Fig. 5d.

This is more clearly illustrated in Fig. 7, which plots the nondimensional out-of-plane deflection of the center point for the $n = 1$ model, w^* in Fig. 5c, against the applied load. For in-plane imperfections, this remains zero. For out-of-plane imperfections only, there is a sudden increase in w^* up to critical buckling, which then diminishes slowly as the tension member stiffens.

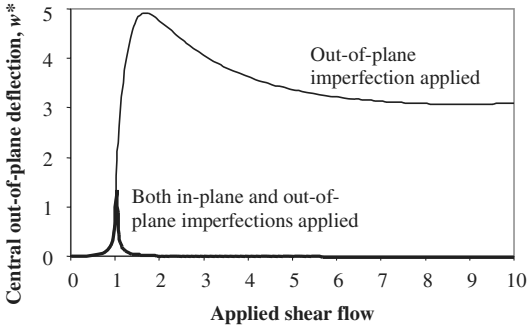

Fig. 7 Out-of-plane deflection for postbuckling of $n = 1$ truss lattice. Shear flow and deflection are nondimensionalized with respect to their critical values.

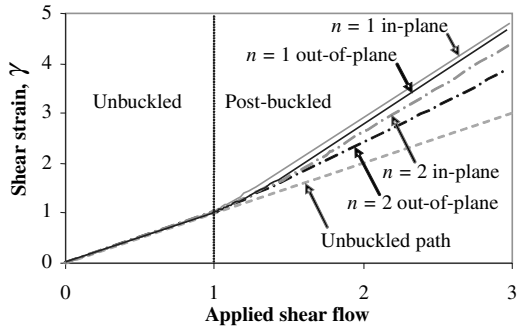

Fig. 8 Shear deformation for $n = 1$ and $n = 2$ truss lattices. Shear flow and shear strain are nondimensionalized with respect to their critical values.

It is interesting to note that when both the in-plane and the out-of-plane imperfections are applied simultaneously, it is the in-plane buckling mode that dominates, with some initial out-of-plane buckling that subsequently reduces to zero, shown in Fig. 7. The preference for in-plane buckling may be due to the energy requirements of the mode shapes. The out-of-plane buckling mode requires additional development past the critical mode shape into a higher mode. The in-plane mode has no such requirements and hence is a lower energy mode.

In the out-of-plane mode for the $n = 2$ model in Fig. 6c, the central compression member A develops into a similar mode as for eigenbuckling, but with a restricted out-of-plane displacement due to the stiffening effect of the central tension member B. The outer compression members C buckle out-of-plane initially, but are subjected to a geometric in-plane displacement during postbuckle. The lattice members are sensitive to the in-plane displacements, and a small difference between the lateral positioning of points D and E is sufficient to initiate an in-plane buckle, hence the combined in-plane and out-of-plane deflections in these members.

The in-plane postbuckled mode shape for the $n = 2$ model in Fig. 6d maintains its initial buckling form. The central compression member develops two sine waves, and the outer compression members take the form of complete sine waves. As for the $n = 1$ model, the tension members act to restrict some rotation at the intersections.

Figure 8 plots the shear deformation of the structure, where γ is the shear strain shown in Fig. 6c, and both γ and shear flow are nondimensionalized with respect to their critical values. In the unbuckled region the deformation is linear, in accordance with Hooke's law. Once the structure begins to buckle, the rate of deformation increases as the load is transferred to the tension members. This change in rate of deformation occurs more gradually as the number of cells in the truss lattice is increased.

The difference in energy requirements between in-plane and out-of-plane modes can also be seen in Fig. 8. A sudden increase in deformation at critical load occurs for in-plane deformation, whereas there is a gradual change for the out-of-plane mode, as the final mode shape has not been fully established when the critical load is reached. This is apparent for the $n = 1$ model, but the effect is even greater for the $n = 2$ model.

Although the optimized truss lattice can deform in either the in-plane or the out-of-plane mode at the same critical load, the structure is not unstable. Even under the presence of imperfections in both modes, only one mode is developed in the postbuckled region. Furthermore, the structure is fundamentally stable, as it can support shear loads in excess of the critical buckling load through transferring additional compression loads to the tension members.

Comparison Between Truss Lattice and Continuous Web

This section compares the structural performance of optimum truss lattices with the traditional continuous-web shear panels of equal area, by considering a range of typical aircraft applications. The finite element models have demonstrated that the truss-lattice design has load transfer characteristics in postbuckling that are similar to the diagonal tension field that develops in a continuous shear panel. However, the lattice could only be considered to be advantageous over the continuous web if it offers the potential for saving weight. It is therefore useful to run a comparison between a postbuckled continuous web and an optimized truss lattice.

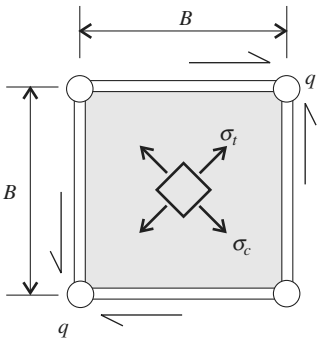

Fig. 9 Continuous-web panel of thickness t.

For the continuous web, shown in Fig. 9, the critical value of shear flow at onset of buckling, q^c, is represented by

$$q^c = \frac{KEt^3}{B^2} \tag{22}$$

where E is the elastic modulus of the web, and K is a coefficient that is dependent upon boundary conditions and aspect ratio [4,22]. For the following study, it shall be assumed that the web has Poisson's ratio of 0.3 and is simply supported with an aspect ratio of one, in which case, $K = 8.4$ [22].

Clearly, the volume of the continuous web is

$$V_w = B^2 t \tag{23}$$

The applied shear flow produces tensile and compressive components of stress within the continuous web, represented by σ_t and σ_c, respectively, in Fig. 9. Before buckling occurs, the two components are equal, and the tensile stress is given by

$$\sigma_w = \sigma_t = \sigma_c = q/t \tag{24}$$

Now, combining Eqs. (23) and (24), it can be seen that

$$\sigma_w = \frac{qB^2}{V_w} \tag{25}$$

If we compare Eq. (25) with Eq. (21), it can be seen that an unbuckled truss lattice has twice the stress of an unbuckled continuous web of the same volume.

Once buckling occurs, the proportion of further applied load carried in compression gradually decreases [4]. For this analysis, the conservative assumption is made that there is no increase in compressive stress beyond q^c, and all additional load is taken in tension. The tensile stress at q can thus be represented by

$$\sigma_w = \frac{q^c}{t} + \frac{2(q - q^c)}{t} \tag{26}$$

Typical values of shear panel dimension and shear load for aircraft wing structures are applied to Eqs. (13–26) to compare the structural efficiency of the truss-lattice configuration with the equivalent continuous web. The $n = 4$ configuration is chosen for this comparison as the benefits are seen to be less significant when $n > 4$ in Fig. 3. The range of structures considered in Table 2 is based on typical loading requirements in aerospace structures of the conventional configuration and vary from a heavily loaded spar at $q = 1$ kN/mm to a lightly loaded rib at $q = 10^{-3}$ kN/mm.

For the postbuckled continuous web, the thickness of the web is the design variable and no additional stiffeners can be introduced. It is assumed that buckling is permitted at 50% of the design shear load, and hence the thickness can be minimized to allow buckling at this

Table 2 A dimensional comparison between continuous and truss-lattice web designs

		Heavy spar	Intermediate values		Light rib
	q, kN/mm	1	10^{-1}	10^{-2}	10^{-3}
	B, m	0.2	0.2	0.2	0.2
	E, GPa	70	70	70	70
	σ_{max}, MPa	500	500	500	500
Postbuckled continuous web	t, mm	3.2	1.5	0.7	0.5[b]
	q^c, kN/mm	0.5	0.5×10^{-1}	0.5×10^{-2}	1.84×10^{-3}
	$V_w(\times 10^3$ mm$^3)$	13.0	60.2	27.9	20.0
	σ_w, MPa	500	100	21	2
Unbuckled truss lattice ($n = 4$)	b, mm	5.15	2.02	1.13	0.64
	d, mm	13.73	5.37	3.02	1.70
	$V_L(\times 10^3$ mm$^3)$	160.0	24.48	7.74	2.45
	σ_L, MPa	500[a]	327	103	33
	q^c, kN/mm	4.27	10^{-1}	10^{-2}	10^{-3}
	V_L/V_w	**1.23**	**0.41**	**0.28**	**0.12**
Postbuckled truss lattice ($n = 4$)	b, mm	5.15	1.85	0.95	0.54[c]
	d, mm	13.73	4.93	2.54	1.43
	$V_L(\times 10^3$ mm$^3)$	160.0	20.63	5.47	1.73
	σ_L, MPa	500[a]	500[a]	219	69
	q^c, kN/mm	4.27	0.71×10^{-1}	0.5×10^{-2}	0.5×10^{-3}
	V_L/V_w	**1.23**	**0.34**	**0.20**	**0.09**

[a]Dimensions of lattice members restricted by maximum stress.
[b]Continuous-web thickness limited by manufacturing constraints, which prevents buckling.
[c]Lattice members approaching minimum thickness.

load. The constraints that are imposed on the design are the minimum-thickness manufacturing constraint of 0.5 mm and the maximum stress of the material σ_{max}, taken as 500 MPa. The panel dimension B is set at 0.2 m for all load cases.

For the unbuckled truss lattice, the cross sections are minimized to reduce the mass of the structure, subject to the maximum stress constraint. Buckling is also a constraint, such that the cross sections must be sufficient to prevent buckling ($q^c \geq q$).

For the postbuckled truss lattice, the dimensions are minimized to reduce the mass while being constrained by the maximum material stress, but buckling is permitted at loads above 50% of the design shear flow. As for the continuous web, the conservative assumption is made that no additional load is taken in the compressive members after buckling occurs. If the effects of bending and twisting are neglected, the tensile stress at q, from Eq. (19), is now represented by

$$\sigma_L = \frac{q^c B}{\sqrt{2}nbd} + \frac{2(q - q^c)B}{\sqrt{2}nbd} \tag{27}$$

It is noted that postbuckling is not permitted for the truss-lattice model of the heavy spar, owing to the large cross section required by the maximum stress limitation. Stress constraints also delay buckling for the $q = 10^{-1}$ kN/mm load case, until beyond 70% of the design shear flow.

The results are summarized in Table 2, which clearly shows the potential weight-saving benefits from replacing continuous webs with truss-lattice webs, in both the unbuckled and postbuckled forms. For example, if the light rib takes the form of a truss lattice permitted to buckle at 50% of the design load, the volume of material would be just 10% of that of a continuous web, which is restricted in thickness by manufacturing constraints. The unbuckled truss lattice also offers very good volume reductions and would be ideal for lightweight composite constructions, where buckling may not be permitted due to potential delamination damage.

However, the truss lattice is not always a suitable replacement for the continuous postbuckled web. Under higher shear loads, such as the heavily loaded spar, the cross-sectional area is limited by the maximum stress of the material, and hence a greater volume of material is required in comparison with a continuous design. In these instances, the continuous panel is a more efficient design than the truss lattice.

Conclusions

The buckling and postbuckling performance of a truss-lattice model under shear loading was investigated using finite element analysis. The nondimensional buckling loads for truss lattices of varying cell dimension were obtained and used in the minimum-mass optimization of the truss lattice. As a result, the structure has coincident in-plane and out-of-plane buckling modes. Although for many structures this might lead to unstable postbuckling behavior, the optimized truss lattice presented in this paper is fundamentally stable, as shear loads in excess of the critical buckling load are supported by transferring additional compression loads to the tensile members. It was also noted that the structure has a postbuckling preference for in-plane buckling, as very slight imperfections in this direction give rise to predominantly in-plane buckling, regardless of the extent of out-of-plane imperfection imposed.

Increasing the number of cells in the truss-lattice model reduces the volume and hence improves the efficiency of the structure, although the benefit becomes less significant for truss lattices with more than 16 cells ($n > 4$). With decreasing volume comes increasing stress, and therefore truss lattices are also more highly stressed. In a comparison with a continuous panel, this stress proved to be a limiting factor in the design of truss lattices under heavy shear loads, and hence the continuous shear panel was found to be more efficient. However, with lower applied loads, the unbuckled truss lattice was found to have significant potential weight savings over the continuous panel, with these savings increasing when buckling is permitted.

A rectangular cross section was used for the members in this preliminary investigation. However, an optimal cross section is likely to be elliptical, and further improvements to the buckling performance of the truss lattice may be attained. The connection to the frame was assumed to be pinned, although in practice, they are likely to be between pinned and clamped. Further work will consider the effect of boundary conditions on the behavior of the truss-lattice structure. Buckling of the combined loading conditions of bending, compression, and shear was studied in [23], but the postbuckling behavior and optimization has yet to be considered. Other factors that may also be considered in future studies include the influence of material type, the interaction with the surrounding structure, the effect of altering the angle of the internal lattice members, and the influence and limitations of manufacturing processes.

Acknowledgments

This research is sponsored by the Innovative Design and Manufacturing Research Centre (IDMRC) in the Department of Mechanical Engineering at the University of Bath, funded by the Engineering and Physical Sciences Research Council (EPSRC).

References

[1] Paul, D., and Pratt, D., "History of Flight Vehicle Structures 1903–1990," *Journal of Aircraft*, Vol. 41, No. 5, 2004, pp. 969–977. doi:10.2514/1.4036

[2] Megson, T. H. G., *Aircraft Structures for Engineering Students*, Butterworth-Heinemann, Oxford, 2002.

[3] Wagner, H., "Flat Sheet Metal Girders with Very Thin Metal Web, Part 3: Sheet Metal Girders with Spars Resistant to Bending. The Stress in Uprights—Diagonal Tension Fields," NACA TM 606, 1931.

[4] Kuhn, P., Peterson, J. P., and Levin, L. R., "A Summary of Diagonal Tension, Part 1: Methods of Analysis," NACA TN-2661, 1952.

[5] Bradshaw, R., Campbell, D., Gargari, M., Mirmiran, A., and Tripeny, P., "Special Structures: Past, Present, and Future," *Journal of Structural Engineering*, Vol. 128, No. 6, 2002, pp. 691–709. doi:10.1061/(ASCE)0733-9445(2002)128:6(691)

[6] Rehfield, L. W., "A Brief History of Analysis Methodology for Grid-Stiffened Geodesic Composite Structures," *Evolving and Revolutionary Technologies for the New Millennium*, Society for the Advancement of Material and Process Engineering, Long Beach, CA, May 1999, pp. 956–964.

[7] Hutchinson, R. G., and Fleck, N. A., "The Structural Performance of the Periodic Truss," *Journal of the Mechanics and Physics of Solids*, Vol. 54, No. 4, 2006, pp. 756–782. doi:10.1016/j.jmps.2005.10.008

[8] Wicks, N., and Hutchinson, J. W., "Optimal Truss Plates," *International Journal of Solids and Structures*, Vol. 38, Nos. 30–31, 2001, pp. 5165–5183. doi:10.1016/S0020-7683(00)00315-2

[9] Despande, V. S., Fleck, N. A., and Ashby, M. F., "Effective Properties of the Octet-Truss Lattice Material," *Journal of the Mechanics and Physics of Solids*, Vol. 49, No. 8, 2001, pp. 1747–1769. doi:10.1016/S0022-5096(01)00010-2

[10] Thompson, J. M. T., and Hunt, G. W., *Elastic Instability Phenomena*, Wiley, London, 1984.

[11] Kim, H., Butler, R., and Williams, P. A., "Buckling and Post-Buckling Analysis of Shear Panels for Optimisation," *Computational Mechanics (WCCM VI)* [CD-ROM], Tsinghua Univ. Press, Beijing, and Springer, New York, Sept. 2004.

[12] Haftka, R. T., and Gurdal, Z., *Elements of Structural Optimization*, Kluwer Academic, Norwell, MA, 1992.

[13] Thompson, J. M. T., and Hunt, G. W., *A General Theory of Elastic Stability*, Wiley, London, 1973.

[14] Tvergaard, V., "Influence of Post-Buckling Behavior on Optimum Design of Stiffened Panels," *International Journal of Solids and Structures*, Vol. 9, No. 12, 1973, pp. 1519–1534. doi:10.1016/0020-7683(73)90057-7

[15] Van der Neut, A., "The Interaction of Local Buckling and Column Failure of Thin Walled Compression Members," *Proceedings of the 12th International Congress of Applied Mechanics*, Springer–Verlag, Berlin, 1969, pp. 389–399.

[16] Olhoff, N., and Seyranian, A. P., "On the Bifurcation and Initial Post-Buckling Behavior of Structures with Bimodal Optimum Buckling Loads," *Computational Mechanics (WCCM VI)* [CD-ROM], Tsinghua Univ. Press, Beijing, and Springer, New York, Sept. 2004.

[17] Timoshenko, S., and Young, D. H., *Elements of Strength of Materials*, 5th ed., D. Van Nostrand, London, 1968, p. 92.

[18] ABAQUS, Software Package, Ver. 6.4, ABAQUS, Inc., Providence, RI, 2003.

[19] Wittrick, W. H., and Williams, F. W., "An Algorithm for Computing Critical Buckling Loads of Elastic Structures," *Journal of Structural Mechanics*, Vol. 1, No. 4, 1973, pp. 497–518.

[20] Williams, P. A., Butler, R., Kim, H. A., and Hunt, G. W., "Complementary Post-Buckling Analyses of Truss-Lattice Shear Panels," 48th AIAA/ASME/ASCE/AHS/ASC Structures, Structural Dynamics and Materials Conference, Honolulu, HI, AIAA Paper 2007-2124, 2007.

[21] Riks, E., "An Incremental Approach to the Solution of Snapping and Buckling Problems," *International Journal of Solids and Structures*, Vol. 15, No. 7, 1979, pp. 529–551. doi:10.1016/0020-7683(79)90081-7

[22] "Structural Design Data—Flat Alloy Plates in Shear," British Aircraft Corp., Bristol, England, U.K., pp. 35.0.1–35.4.5, 1972.

[23] Kim, H. A., Featherston, C. A., Ussel, J., and Williams, P. A., "Introducing a Discrete Modelling Technique for Buckling of Panels Under Combined Loading," *Structural and Multidisciplinary Optimization* (to be published).

J. Cooper
Associate Editor